Food Hydrocolloids 23 (2009) 2425–2433

Contents lists available at ScienceDirect

Food Hydrocolloids

journal homepage: www.elsevier.com/locate/foodhyd

Ferrous bisglycinate content and release in $W_1/O/W_2$ multiple emulsions stabilized by protein–polysaccharide complexes

R. Jiménez-Alvarado [a], C.I. Beristain [b], L. Medina-Torres [c], A. Román-Guerrero [a], E.J. Vernon-Carter [d,*]

[a] Departamento de Biotecnología, Universidad Autónoma Metropolitana-Iztapalapa, San Rafael Atlixco 186, Col. Vicentina, CP 09340 México, DF, Mexico
[b] Instituto de Ciencias Básicas, Universidad Veracruzana, Av. Dr. Rafael Sánchez el Altamirano s/n Km, 3.5 carreteras Xalapa-Las Trancas, Coronel Industrial Las Animas, CP 91192, Xalapa, Veracruz, Mexico
[c] Facultad de Química, Conjunto E, L213, Ingeniería Química, Universidad Nacional Autónoma de México, CP 04510 Ciudad de México, DF, Mexico
[d] Departamento de Ingeniería de Procesos e Hidráulica, Universidad Autónoma Metropolitana-Iztapalapa, San Rafael Atlixco 186, Col. Vicentina, Edificio T-247, CP 09340 México, DF, Mexico

ARTICLE INFO

Article history:
Received 16 March 2009
Accepted 29 June 2009

Keywords:
Multiple emulsions
Ferrous bisglycinate
Protein:polysaccharide complexes
Release kinetics
Protection against oxidation

ABSTRACT

Ferrous bisglycinate aqueous solution was entrapped in the inner phase (W_1) of water-in-oil-in-water ($W_1/O/W_2$) multiple emulsions. The primary ferrous bisglycinate aqueous solution-in-mineral oil (W_1/O) emulsion contained 15% (w/w) ferrous bisglycinate, had a dispersed phase mass fraction of 0.5, and was stabilized with a mixture of Grindsted PGPR 90:Panodan SDK (6:4 ratio) with a total emulsifiers concentration of 5% (w/w). This primary emulsion was re-emulsified in order to prepare $W_1/O/W_2$ multiple emulsions, with a dispersed mass fraction of 0.2, and stabilized using protein (whey protein concentrate (WPC)):polysaccharide (gum arabic (GA) or mesquite gum (MG) or low methoxyl pectin (LMP)) complexes (2:1 ratio) in the W_2 aqueous phase. The $W_1/O/W_2$ multiple emulsion stabilized with WPC:MG (5% w/w total biopolymers concentration) provided smaller droplet sizes (2.05 μm), lower rate of droplet coalescence (7.09×10^{-7} s^{-1}), better protection against ferrous bisglycinate oxidation (29.75% Fe^{3+}) and slower rate of ferrous bisglycinate release from W_1 to W_2 ($K_H = 0.69$ mg mL^{-1} $min^{-0.5}$ in the first 24 h and 0.07 mg mL^{-1} $min^{-0.5}$ for the next 19 days of storage time). Better encapsulation efficiencies, enhanced protection against oxidation and slower release rates of ferrous bisglycinate were achieved as the molecular weight of the polysaccharide making up protein:polysaccharide complex was higher. Thus, the factor that probably affected most the overall functionality of multiple emulsions was the thickness of the complex adsorbed around the multiple emulsion oil droplets. These thicknesses determined indirectly by measuring the z-average diameter of the complexes, and that of the WPC:MG (529.4 nm) was the largest.

© 2009 Elsevier Ltd. All rights reserved.

1. Introduction

Ferrous bisglycinate has a great potential as food fortificant because its absorption in humans is not limited by action of phytates or polyphenols. The supplementation of ferrous bisglycinate is usually made by incorporating it directly as a solution in food systems, but two inconveniences occur: (1) ferrous bisglycinate interacts with other food components changing the taste of foods, which is detected by consumers, and (2) it is oxidized easily (Bovell-Benjamin, Viteri, & Allen, 2000). Thus, an actual research challenge is how to incorporate ferrous bisglycinate in food systems in order to diminish or delete these negative effects. One possibility is to entrap ferrous bisglycinate in the inner aqueous phase of a water-in-oil-in-water ($W_1/O/W_2$) multiple emulsion. $W_1/O/W_2$ emulsions consist of water droplets dispersed within larger oil droplets, which are on turn dispersed in an aqueous continuous phase (McClements, 2005). A boost in their use has occurred recently in diverse fields such as water treatment (Pimentel-González, Revah, Campos-Montiel, Monroy-Hermosillo, & Vernon-Carter, 2008), foods (Dickinson & McClements, 1996; Lobato-Calleros, Rodriguez, Sandoval-Castilla, Vernon-Carter, & Alvarez-Ramirez, 2006; Lobato-Calleros et al., 2008; Muschiolik, 2007), natural colorants protection (Rodríguez-Huezo, Pedroza-Islas, Prado-Barragán, Beristain, & Vernon-Carter, 2004), and cosmetics (Bais & Lapasin, 2003), due to improvements in their stability, primarily through the use of biopolymers as stabilizing agents in the outer aqueous phase. Protein–hydrocolloid interactions play a significant role in the structure and stability of many processed foods, and the control of these macromolecular interactions is a key factor in the development of novel food processes and products (Lutz, Aserin, Portnoy, Gottlieb,

* Corresponding author. Tel.: +52 55 5804 4648; fax: +52 55 5804 4900.
E-mail address: jvc@xanum.uam.mx (E.J. Vernon-Carter).

0268-005X/$ – see front matter © 2009 Elsevier Ltd. All rights reserved.
doi:10.1016/j.foodhyd.2009.06.022

& Garti, 2009), including multiple emulsions. These biopolymers can chemically interact through covalent bonds or physically through electrostatic interactions (Dickinson, 2008; Ettelaie, Akinshina, & Dickinson, 2008). These interactions can be attractive or repulsive, weak or strong, and specific or non specific (Tolstoguzov, 1998). In systems as $W_1/O/W_2$ multiple emulsions, containing several surface-active components, three types of adsorption mechanisms at the interface have been described: a) competitive adsorption, b) associative adsorption, and c) layered adsorption (Bergenståhl, 1995).

$W_1/O/W_2$ emulsions with improved stability and homogeneity in droplet size distribution were prepared by using protein:polysaccharide (Pr:Ps) complexes at the external oil–water interface (Benichou, Aserin, & Garti, 2002). Electrostatic complexation between biopolymers at the external interface led to a better coverage of the interface, and to an enhanced stabilization of the $W_1/O/W_2$ emulsions against aggregative mechanisms through steric effects. Pr:Ps complexation depends on the relative concentrations and ratios between the biopolymers (Benichou et al., 2002; Espinosa-Andrews, Báez-González, Cruz Sosa, & Vernon-Carter, 2007; Weinbreck, Nieuwenhuijse, Robjin, & de Kruif, 2003; Weinbreck, Tromp, & de Kruif, 2004). Furthermore, these variables influence, to a large extent, the structural and mechanical properties of multicomponent food systems (Tolstoguzov, 1990).

Studies on the release kinetics of $W_1/O/W_2$ emulsions have been done for magnesium (Bonnet et al., 2009) showing that the release kinetics seemed to be determined by diffusion and/or permeation mechanisms. Pimentel-González et al. (2008) used double emulsions with a microbial consortium entrapped in the inner aqueous phase for degrading methyl *tert*-butyl ether (MTBE) contained in the outer aqueous phase. The emulsifier dissolved in the oil phase helped to transport the MTBE from the outer to the inner aqueous phase. This type of diffusion is known as facilitated transport, and can work in the reverse direction for leaching out a material contained in the inner aqueous phase (Kralj & Brečević, 1998).

The aim of this work was to entrap ferrous bisglycinate in the inner aqueous phase (W_1) of $W_1/O/W_2$ emulsions stabilized by protein:polysaccharide complexes in the outer aqueous phase (W_2) and to determine the effect of the relative concentrations and ratios between the biopolymers, and the pH where electrostatic complexation is maximized on: (a) $W_1/O/W_2$ emulsions droplet size and stability; (b) ferrous bisglycinate encapsulation yield; (c) ferrous bisglycinate protection against oxidation; and (d) release kinetics of ferrous bisglycinate from the inner aqueous phase to the outer aqueous phase of the multiple emulsions.

2. Materials and methods

Ferrous bisglycinate powder was provided by UNIPHARM de Mexico, S.A. de C.V. (State of Veracruz, Mexico), containing 18–20% of elemental iron. Mineral oil (NF-85 food grade from Materiales y Abastos Especializados, S.A. de C.V., Mexico, D.F., Mexico) was used as the oil phase (O) of the $W_1/O/W_2$ multiple emulsions. The water-soluble surfactant (WS) (Panodan SDK, esters of monoglycerides and diglycerides of diacetyl tartaric acid) and the oil-soluble surfactant (OS) (Grindsted PGPR 90, esters of polyglycerol and polyricinoleate fatty acids) were purchased from Danisco Mexico, S.A. de C.V. Mesquite gum (MG) tears were hand collected in the Mexican State of San Luis Potosi, Mexico, were pulverized in a Bicor mill and, in order to stop enzymatic activity, dissolved in water at 77 °C for 1 h in a Polinox jacketed vessel with a propeller type agitator, filtered with high-flow supercel in a Shriver filter press and dried in a Bowen BLSA spray-drier with an inlet temperature of 175 °C (Vernon-Carter et al., 1996). Low methoxyl pectin (LMP) (Grindsted LC-950) was provided by Dannova Quimica, S.A. de C.V. (Mexico, D.F., Mexico). Gum arabic (GA) was purchased from Sigma–Aldrich Quimica S.A. de C.V. (Toluca, State of Mexico, Mexico). Whey protein concentrate (WPC; Hilmar 8000) containing 80% protein in dry basis was acquired from Hilmar Ingredients (Hilmar, CA, USA). Analytical reagents used for the determination of iron were: α,α'-bipiridyl purchased from Sigma–Aldrich Quimica S.A. de C.V. (Toluca, State of Mexico, Mexico), ascorbic acid purchased from Tecsiquim S.A. de C.V. (Toluca, State of Mexico, Mexico), standard iron powder (99.99%), anhydrous sodium acetate purchased from Productos Quimicos Monterrey, S.A. (Monterrey, State of Nuevo Leon, Mexico), and glacial acetic acid purchased from J.T. Baker, S.A. de C.V. (Xalostoc, State of Mexico, Mexico). Deionized water was used in all the experiments, and sodium azide (Hycel de Mexico, S.A. de C.V., Mexico, D.F., Mexico) was used as preservative.

2.1. Preparation of emulsions

$W_1/O/W_2$ multiple emulsions were prepared at 25 °C using a two-stage emulsification procedure (Rodríguez-Huezo et al., 2004).

2.1.1. Formulation of W_1/O emulsions

In the first stage, 0.5 dispersed phase mass fraction ($\varphi_{W1/O}$) water-in-oil (W_1/O) primary emulsions were prepared, with different total surfactant concentrations (6, 8, 10, 12 and 14% w/w), and OS:WS ratios (9:1, 8:2, 7:3, 6:4, and 5:5). The primary emulsions were coded as $(W_1/O)_{x,y}$, where the subscript x denotes the total surfactants concentration, and subscript y denotes the OS:WS ratio. In all the cases a 30% (w/w) ferrous bisglycinate aqueous solution (W_1) was dripped into the oil phase (O) homogenizing by means of sonication (Sonics Vibra Cell VCX 130 PB, Sonics & Materials, Inc., Newtown, CT, USA) at 70% amplitude and frequency of 20 kHz for 15 min.

2.1.1.1. Rate of coalescence of $(W_1/O)_{x,y}$ emulsions. The droplet sizes of the $(W_1/O)_{x,y}$ emulsions were determined with a Malvern Mastersizer 2000 (Malvern Instruments Ltd., Malvern, Worcestershire, U.K.), using commercial soy oil (refractive index 1.475) as dispersant. The number volume mean diameter ($d_{3,0}$) of the $(W_1/O)_{x,y}$ emulsions was determined over time. The rate of coalescence ($K_{C\,(W1/O)x,y}$) of the primary emulsions was determined as reported by Ruíz-Ramos et al. (2006). The primary emulsion that had the lowest rate of coalescence was selected for formulating the multiple emulsions.

2.2. Conditions leading to the formulation of $W_1/O/W_2$ multiple emulsions

Prior to formulating the $W_1/O/W_2$ multiple emulsions, the zeta potential of the individual biopolymers solutions, the yield and composition of the Pr:Ps complexes were determined, and this information was used for establishing the usage conditions to be used in W_2.

2.2.1. Zeta potential

Aqueous solutions 5% (w/w) of WPC, GA, MG, and 2% (w/w) LMP were prepared and stored at 4 °C during 24 h in order to allow their complete hydration. The zeta potential of the biopolymers aqueous solutions was determined at different pH values using a Malvern Zetasizer Nano ZS (Malvern Instruments Ltd., Malvern, Worcestershire, UK). pH of aqueous solutions of biopolymers was adjusted by the addition of 0.1N HCl and/or 0.1N NaOH. The pH where the maximum stoichiometric difference of the electrostatic charges between protein and polysaccharide occurred (pH_E) was determined.

2.2.2. Protein:polysaccharide complexation, coacervate yield and z-average diameter

Solutions of binary mixtures of biopolymers (Pr:Ps) were prepared at different total biopolymers concentrations (from 1 to 10% (w/w)) for the WPC:GA and WPC:MG mixtures, and from 0.4 to 1.6% (w/w) for the WPC:LMP mixture and at different ratios (0.5:1 to 4:1), and stored for 24 h at 4 °C in order to allow their complete hydration. The pH of these solutions was adjusted in a range from 1.5 to 5 using 0.1N HCl, and monitored to determine if Pr:Ps complexes were formed through their precipitation (complex coacervates). These biopolymers solutions were stored during 48 h at 4 °C. The complex coacervates were dehydrated at 45 °C in an oven until constant weight was achieved. The coacervate yield was calculated with the following equation:

$$\%\mathrm{RC} = \frac{m_C}{m_{BP}} \times 100 \quad (1)$$

where %RC is the coacervate yield, m_{BP} is the total mass of the biopolymers used in the preparation of the binary mixtures, and m_C is the mass of the dehydrated complex coacervate.

Additionally, the z-average diameter of the Pr:Ps complexes, previous to their dehydration, was determined by means of laser light scattering using Malvern Zetasizer Nano ZS, as indirect method for providing information regarding the thickness of the adsorbed biopolymer layers around the oil droplets of the multiple emulsions.

2.2.3. Composition of the protein:polysaccharide complexes

Elemental composition of the complex coacervates was determined using an elemental analysis equipment PE2400 series II CHNS/O (Perkin–Elmer, USA), calculating the total carbon, hydrogen, and nitrogen concentrations in the Pr:Ps complexes samples, using the nitrogen concentration as differential element between the protein and the polysaccharides used. The quantity of polysaccharide in the coacervate was calculated from the following equation:

$$\%\mathrm{POLYSACCHARIDE} = \frac{\%N_C - \%N_{WPC}}{\%N_{PS} - N_{WPC}} \times 100 \quad (2)$$

where $\%N_C$, $\%N_{WPC}$, and $\%N_{PS}$, are the nitrogen concentrations found in the Pr:Ps complexes, in WPC, and in the polysaccharides used respectively.

2.2.4. Formulation of $(W_1/O/W_2)_{a,b,c}$ multiple emulsions

The $(W_1/O)_{x,y}$ primary emulsion with the lowest $K_{C(W1/O)x,y}$ was re-emulsified in aqueous binary mixtures of biopolymers (WPC:GA, WPC:GM, and WPC:LMP) producing $(W_1/O/W_2)_{a,b,c}$ multiple emulsions, where the subscript *a* denotes the total biopolymers concentration, the subscript *b* denotes the Pr:Ps ratio, and the subscript *c* denotes the mixture of biopolymers. Total concentration and ratio of biopolymers used for formulating the $(W_1/O/W_2)_{a,b,c}$ multiple emulsions was established from the results of coacervate yield. Thus, the three following emulsions $(W_1/O/W_2)_{5\%,2:1,WPC:GA}$, $(W_1/O/W_2)_{5\%,2:1,WPC:MG}$, and $(W_1/O/W_2)_{0.7\%,2:1,WPC:LMP}$ were produced. The re-emulsification of the primary emulsion was made by dripping it into the mixture of biopolymers, homogenizing by means of sonication (Sonics Vibra Cell VCX 130 PB, Sonics & Materials, Inc., Newtown, CT, USA) at 50% amplitude and frequency of 20 kHz for 15 min. The dispersed phase mass fraction in the $(W_1/O/W_2)_{a,b,c}$ emulsion ($\varphi_{W1/O/W2}$) was 0.2 in all the cases. Immediately after the emulsion was formed, the pH of multiple emulsions was adjusted to the pH where the formation of Pr:Ps complexes was maximized (pH_C), using 0.1N HCl in order to allow the formation of a biopolymeric complex at the outer oil–water interface.

2.2.5. Rate of coalescence of $(W_1/O/W_2)_{a,b,c}$ multiple emulsions

The rate of coalescence of $(W_1/O/W_2)_{a,b,c}$ multiple emulsions ($K_{C(W1/O/W2)a,b,c}$), was determined using the methodology described in Section 2.1.1.1, but using water instead of oil as dispersant. Additionally the span of the $(W_1/O/W_2)_{a,b,c}$ multiple emulsions, a dimensionless width parameter that can provide a relative measure the polydispersity of the emulsions droplet size was determined.

2.3. Protective effect of the $(W_1/O/W_2)_{a,b,c}$ multiple emulsions against ferrous bisglycinate oxidation

The ferrous iron (Fe^{2+}), total iron, and ferric iron (Fe^{3+}) contents were determined spectrophotometrically (AOAC, 1995, chap. 18). 10 mL of the $(W_1/O/W_2)_{a,b,c}$ multiple emulsion were dissolved in HCl (0.2% v/v) and diluted with water in order to achieve a concentration of ~3 mg of total iron per 100 mL. Fe^{2+} content was determined by its complexation with α,α′–bipiridyl at pH 4.5 and measuring the absorbance at 523 nm using a spectrophotometer (Spectronic Genesys2, Thermo Fisher Scientific, Waltham, MA., USA). Total iron content was determined by reducing Fe^{3+} with ascorbic acid to Fe^{2+}, and complexing it with α,α′–dipiridyl. Fe^{3+} content was determined by the difference between total iron minus Fe^{2+} along 480 h.

2.3.1. Encapsulation yield and release kinetics

W_2 was separated from $(W_1/O/W_2)_{a,b,c}$ emulsion by centrifugation at 1500 rpm for 15 min at 4 °C using a HERMLE Z323K high-speed centrifuge (Hermle, Labortechnic, Germany). Total iron in W_2 was quantified during storage time, as a measure of the release kinetics of ferrous bisglycinate.

Encapsulation yield was determined with the following equation:

$$\mathrm{EY} = \frac{\mathrm{Fe}_{(W_1/O/W_2)} - \mathrm{Fe}_{W_2}}{\mathrm{Fe}_{(W_1/O/W_2)}} \times 100 \quad (3)$$

where EY is the ferrous bisglycinate encapsulation yield percentage, $Fe_{(W1/O/W2)}$ is the total iron present in the whole $(W_1/O/W_2)_{a,b,c}$ emulsion, and Fe_{W2} is the total iron present in W_2. EY was determined for fresh samples and for samples after 20 days of storage.

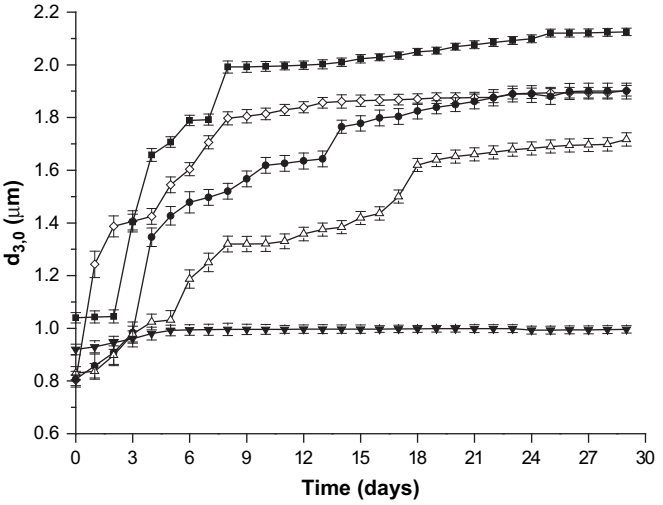

Fig. 1. Change in the number volume mean diameter ($d_{3,0}$) of $(W_{1/O})_{x,y}$ primary emulsions: $(W_{1/O})_{10\%,9:1}$ (◇); $(W_{1/O})_{10\%,8:2}$ (●); $(W_{1/O})_{10\%,7:3}$ (△); $(W_{1/O})_{10\%,6:4}$ (▼); and $(W_{1/O})_{10\%,5:5}$ (■) primary emulsions over time.

Table 1
Coalescence rates ($K_{C(W1/O)x,y}$) of the $(W_1/O)_{x,y}$ primary emulsions, subscript x denotes total surfactant concentration and subscript y denotes OS:WS ratio.

$(W_1/O)_{x,y}$		$K_{C(W1/O)x,y}$
x	y	(s^{-1})
6	9:1	1.15×10^{-5} b
	8:2	1.23×10^{-5} a
	7:3	1.45×10^{-5} a
	6:4	1.91×10^{-6} d
	5:5	1.82×10^{-6} c
8	9:1	1.81×10^{-6} c
	8:2	1.87×10^{-6} c
	7:3	1.85×10^{-6} c
	6:4	1.47×10^{-6} d
	5:5	1.84×10^{-6} c
10	9:1	6.51×10^{-7} f
	8:2	9.52×10^{-7} e
	7:3	9.16×10^{-7} e
	6:4	2.52×10^{-7} g
	5:5	8.99×10^{-7} e
12	9:1	6.72×10^{-7} f
	8:2	9.48×10^{-7} e
	7:3	9.20×10^{-7} e
	6:4	2.53×10^{-7} g
	5:5	9.12×10^{-7} e
14	9:1	9.45×10^{-7} e
	8:2	5.52×10^{-7} f
	7:3	4.16×10^{-7} f
	6:4	2.52×10^{-7} g
	5:5	3.95×10^{-7} f

Values in the same column bearing different letters are significantly different ($P < 0.05$).

The release kinetic of ferrous bisglycinate from W_1 to W_2 phase of the multiple emulsions was fitted to the following models:

$$\text{Hixson \& Crowell model}: \left(1 - \left[Fe_{W_2}\right]/\left[Fe_{W_2}\right]_0\right)^{1/3} = -K_{HC}t + 1 \quad (4)$$

$$\text{Peppas-Higuchi model}: \left[1 - Fe_{W_2}\right]/\left[Fe_{W_2}\right]_0 = K_{PH}t^n \quad (5)$$

$$\text{Jorgensen \& Christensen model}: \left[Fe_{W_2}\right]/\left[Fe_{W_2}\right]_0 = 1 - \left[(1-n)K_J(t-t_0)\right]^{1/(1-n)} \quad (6)$$

$$\text{Zero-order model}: \left[Fe_{W_2}\right] = \left[Fe_{W_2}\right]_0 - K_0 t \quad (7)$$

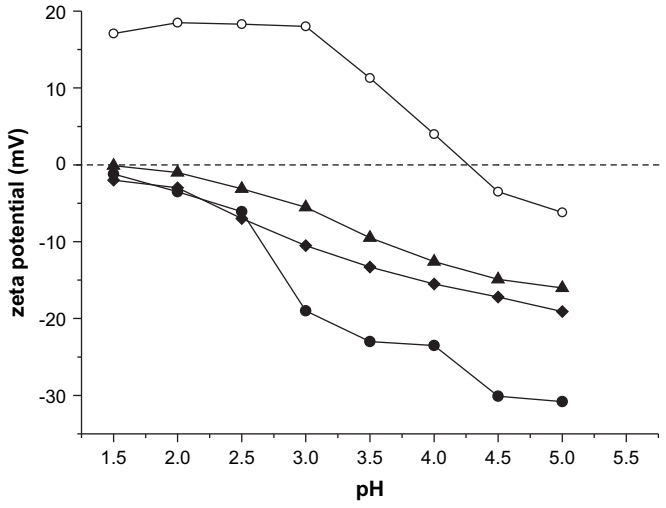

Fig. 2. Zeta potential in function of pH for biopolymers solutions: (○) WPC; (◆) GA; (▲) MG; (●) LMP.

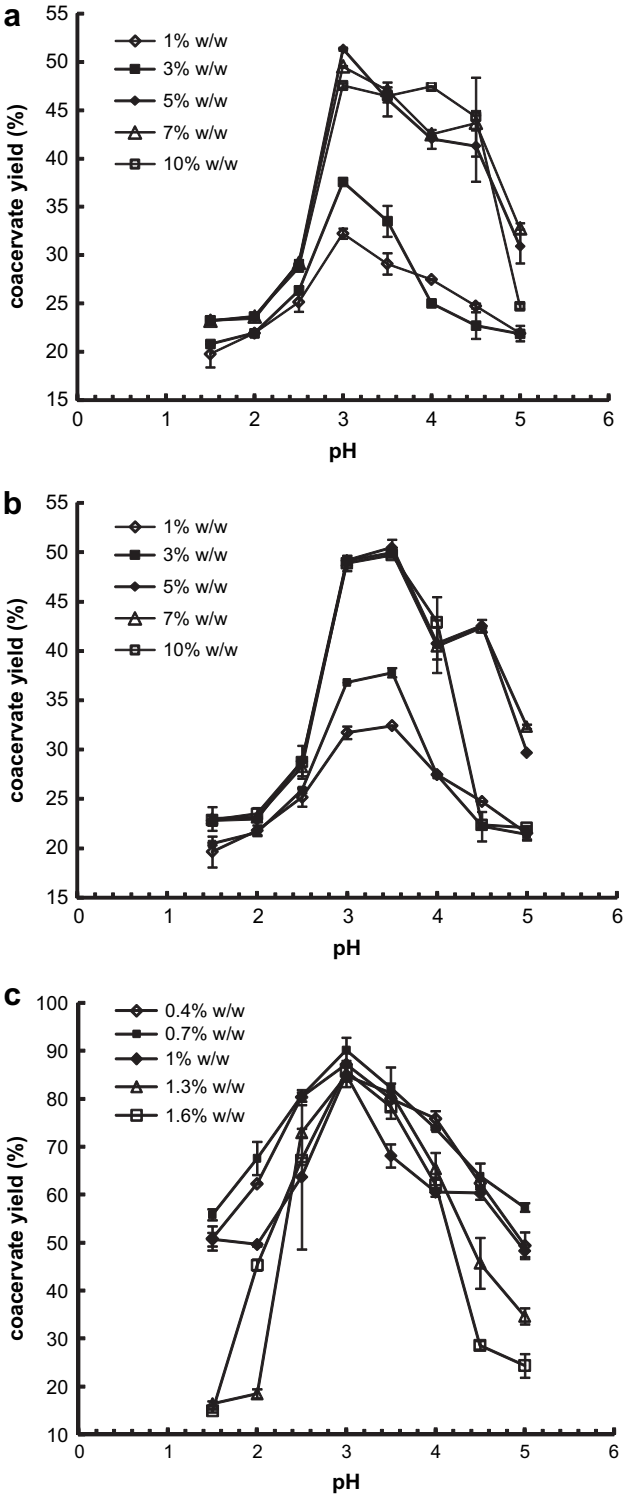

Fig. 3. Coacervate yield based on the pH value and total biopolymers concentration for the binary systems: a) WPC:GA, b) WPC:MG, and c) WPC:LMP in a 2:1 ratio, respectively.

$$\text{First-order model}: \ln\left[Fe_{W_2}\right] = \ln\left[Fe_{W_2}\right]_0 - K_1 t \quad (8)$$

$$\text{Second-order model}: 1/\left[Fe_{W_2}\right] = 1/\left[Fe_{W_2}\right]_0 + K_2 t \quad (9)$$

$$\text{Higuchi's model}: \left[Fe_{W_2}\right] = K_H t^{1/2} \quad (10)$$

where $[Fe_{W2}]$ is the concentration of total iron in W_2 at time t, $[Fe]_0$ is the initial concentration of total iron in W_2, n is a fitting parameter and K_{HC}, K_{PH}, K_J, K_0, K_1, K_2, and K_H are release rate constants.

2.4. Statistical analysis

Data were analyzed using a one way analysis of variance (ANOVA) and a Tukey test for a statistical significance $p \leq 0.05$, using the software NCSS 2000 (Kaysville, Utah, USA). All experiments were done in duplicate.

3. Results and discussion

3.1. Characterization of the $(W_1/O)_{x,y}$ primary emulsion

The effect of OS:WS ratio on $d_{3,0}$ of the $(W_1/O)_{x,y}$ primary emulsions manufactured with a total biopolymer concentration of 10% ($x = 10\%$) with time is shown in Fig. 1. Similar behavior was observed for total surfactant concentrations of 6, 8, 12 and 14% (data not shown). The $d_{3,0}$ of fresh primary emulsions varied from 0.8 to 2 μm, increasing as the OS concentration decreased (Fig. 1). After 30 days of storage at room temperature, $d_{3,0}$ of the primary emulsions increased significantly when prepared with a total surfactant concentration lower than 9% (w/w). The $K_{C(W1/O)x,y}$ did not vary significantly when total surfactant concentration was higher than 10% (w/w), indicating that the emulsions had a good stability against droplet coalescence in accordance to the criteria established by Kitchener and Mussellwhite (1969). The $K_{C(W1/O)x,y}$ of the most stable $(W_1/O)_{x,y}$ primary emulsions are shown in Table 1. Lowest $K_{C(W1/O)x,y}$ was achieved with a 6:4 OS:WS ratio and 10% total surfactant concentration. Increasing the surfactants concentration above 10% did not produce significantly lower $K_{C(W1/O)x,y}$ so that the $(W_1/O)_{10\%,6:4}$ primary emulsion was used as the dispersed phase in the elaboration of the $W_1/O/W_2$ multiple emulsions.

3.2. Effect of pH, concentration, and ratio of biopolymers on the coacervate yield

As can be seen in Fig. 2, the isoelectric point (pI) of the WPC was 4.3 (ionic strength ~0.02), whereas the pH value at which the polysaccharides (GA, MG, LMP) lost the capacity to ionize their carboxyl groups was near to 1.5 (ionic strength ~0.04). Similar values have been reported for GA and whey protein (WP) by Weinbreck, Wientjes, Nieuwenhuijse, Robjin, and de Kruif (2004). Interactions between WPC and the polysaccharides were established through zeta potential sweeps of the biopolymeric solutions in a pH range from 1.5 to 5. The pH_E varied depending on the type of polysaccharide used, resulting a pH_E of 3.0 for WPC:GA, 3.5 for WPC:MG, and 3.0 for WPC:LMP (Fig. 2). Independently of the total biopolymer concentrations used, the pH of maximum coacervate yield (pH_C) for each Pr:Ps binary mixture occurred at the same values at which pH_E occurred, i.e., 3.0 for WPC:GA, 3.5 for WPC:MG, and 3.0 for WPC:LMP (Fig. 3). From Fig. 3 we can also observe that the maximum coacervate yield for the binary mixtures WPC:GA (51.35%) and WPC:GM (50.59%) occurred at a total biopolymer concentration of 5% (w/w). When the total biopolymer concentration decreased to 3% and 1% (w/w), the total coacervate yield decreased significantly, but remained practically constant as it increased to 7% and 10% (w/w) (Fig. 3a, b). The effect of total biopolymer concentration on coacervate yield can probably be best explained in terms of the polyelectrolyte behavior of macromolecules (Pasika, 1977). Ionization of the attached function aids in the solubilization of the polyelectrolyte, which dissolves to yield a polyion and counterions. The polyion holds a large number of charges in close proximity because they are attached to the macromolecular backbone, and although the polyion has mobility, the individual charges attached to the chain do not. Not all of the counterions are free to move about. The free ions form a counterion cloud about the polyion, whereas the immobilized ions are bound to a specific site or point of the macromolecular backbone. As the polyelectrolyte solution is diluted, more and more of the site-bound counterions are released, building the charge of the macro ion,

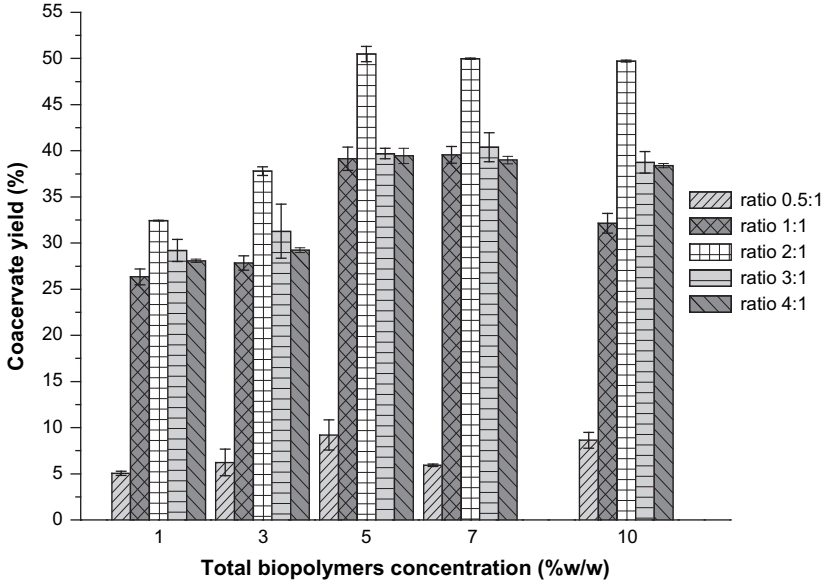

Fig. 4. Coacervate yield based on the ratio between biopolymers and total biopolymers concentration of WPC:MG at pH = 3.5 in the outer aqueous phase of the multiple emulsions.

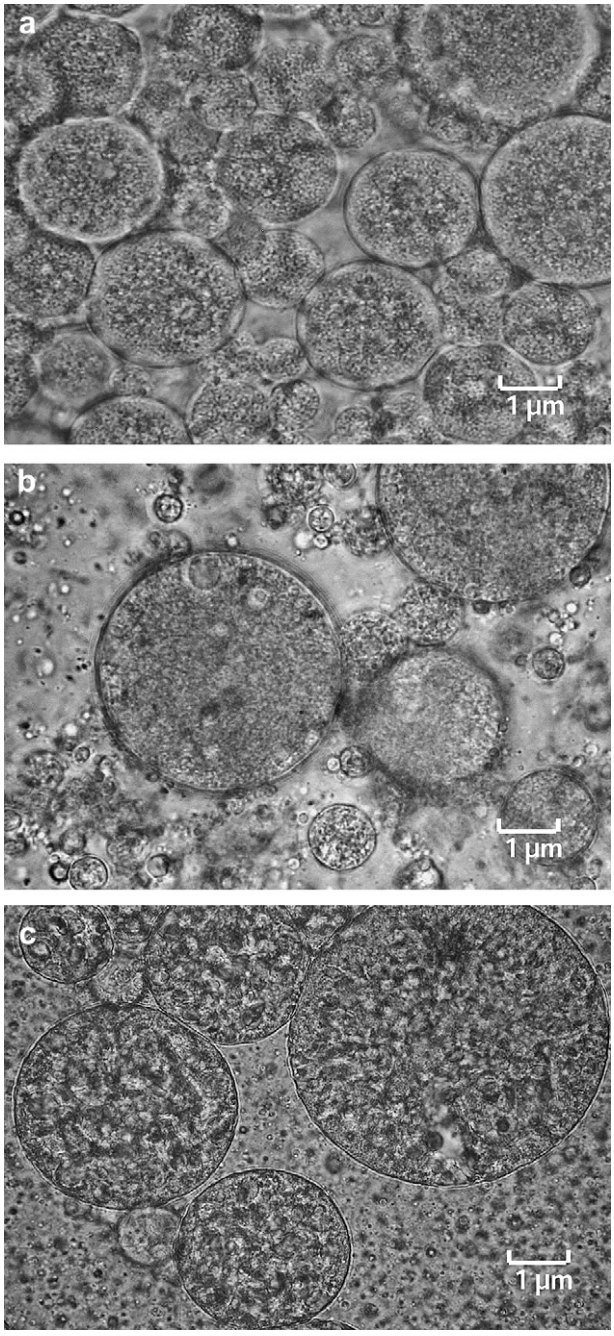

Fig. 5. Micrographs of $(W_1/O/W_2)$ multiple emulsions containing ferrous bisglycinate, stabilized with whey protein concentrate (WPC):mesquite gum(GM) (2:1 ratio; 5% w/w) complex: a) immediately after to be prepared, b) after 2 days, and c) after 20 days of storage time.

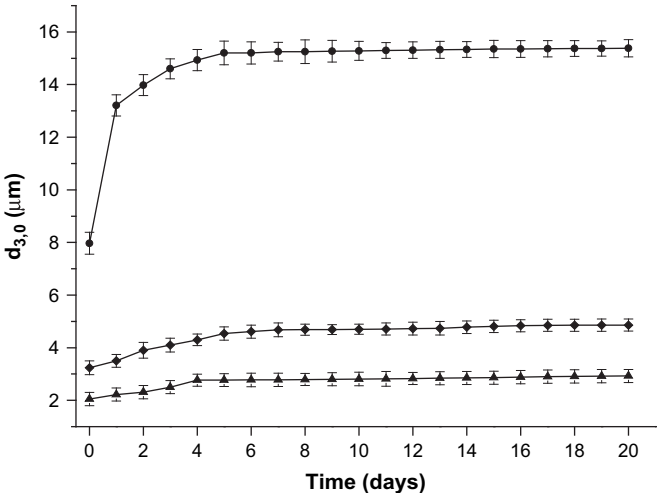

Fig. 6. Change in the number volume mean diameter ($d_{3,0}$) of: $(W_1/O/W_2)_{5\%,2:1,WPC:GA}$ (◆); $(W_1/O/W_2)_{5\%,2:1,WPC:MG}$ (▲); and $(W_1/O/W_2)_{0.7\%,2:1,WPC:LMP}$ (●) multiple emulsions over time.

which expands. Expansion on dilution cannot occur indefinitely, due to flexibility constraints in the macromolecular backbone. The more expanded is the polyion, the higher is the "stiffness" of the macromolecular backbone and the exposed charged sites possess less freedom for interaction. This phenomenon, in addition to the fact that the numbers of polyions available in diluted systems are lower explain the sharp decrease in coacervate yield at low biopolymers concentrations. At relatively high biopolymers concentrations, the degree of ionization of the macromolecule is lower, and the flexibility of the macromolecular backbone is much higher as it is less expanded, so that the charged sites are more readily available for interaction, thus resulting in higher coacervate yields. These results are important in that they pinpoint that neither too low nor high total biopolymers concentrations allow for an efficient coacervate formation (Espinosa-Andrews et al., 2007).

The maximum coacervate yield for the binary mixture WPC:LMP (90.21%) happened at 0.7% (w/w) (Fig. 3c), which was almost as twice better as the best concentrations (5–10%) for the WPC:MG and WPC:GA mixtures (Fig. 3a, b). These coacervate yield differences can be attributed to the differing macromolecular structures of the polysaccharides. While MG and GA consist of a mixture of highly branched arabinogalactan heteropolymers (Fenyo & Vandevelde, 1990; Vernon-Carter, Beristain, & Pedroza-Islas, 2000), LMP dominant's feature is a linear chain of α-(1 → 4)-linked D-galacturonic acid units with varying proportions of the acid groups present as methoxyl (methyl) esters (Voragen, Pilnik, Thibault, Axelos, & Renard, 1995). The linear macro ion (LMP) continues to expand in the absence of structural limitation, compared to the branched species (MG and GA) which reach a limit of expansion earlier because of their structural makeup (Pasika, 1977). Thus, LMP has a greater capability for interaction.

Table 2
Droplet size at zero time and $K_{C(W1/O/W2)a,b,c}$ of the $(W_1/O/W_2)_{a,b,c}$ multiple emulsions.

Multiple emulsions $(W_1/O/W_2)_{a,b,c}$			$d_{3,0}$ Fresh $(W_1/O/W_2)_{a,b,c}$ multiple emulsions (μm)	Span (dimensionless)	$K_{C(W1/O/W2)a,b,c}$ after 20 days of storage (s^{-1})
a	*b*	*c*			
5.0%	2:1	WPC:GA	$3.24 \pm 0.08_b$	$3.85 \pm 0.04_b$	$8.16 \times 10^{-7}{}_b$
5.0%	2:1	WPC:MG	$2.05 \pm 0.07_a$	$1.70 \pm 0.03_a$	$7.09 \times 10^{-7}{}_a$
0.7%	2:1	WPC:LMP	$7.97 \pm 0.39_c$	$8.79 \pm 0.18_c$	$1.25 \times 10^{-6}{}_c$

Values in the same column bearing different letters are significantly different ($P < 0.05$).

Table 3
Change in the amount of Fe^{2+} and Fe^{3+} across the time and encapsulation yield for the whole $(W_1/O/W_2)_{a,b,c}$ multiple emulsions, and loss of total iron in W_1 after 480 h of storage time.

Time (h)	$(W_1/O/W_2)_{5\%,2:1,WPC:GA}$		$(W_1/O/W_2)_{5\%,2:1,WPC:MG}$		$(W_1/O/W_2)_{0.7\%,2:1,WPC:LMP}$	
	Fe^{2+} from total iron (%)	Fe^{3+} from total iron (%)	$Fe^{2+}$from total iron (%)	$Fe^{3+}$from total iron (%)	$Fe^{2+}$from total iron (%)	$Fe^{3+}$from total iron (%)
0	$60.38 \pm 0.51_{f,A}$	$39.62 \pm 0.51_{a,B}$	$89.88 \pm 0.65_{h,B}$	$10.12 \pm 0.65_{a,A}$	$92.01 \pm 1.60_{g,B}$	$7.99 \pm 1.60_{a,A}$
48	$59.12 \pm 0.70_{f,B}$	$40.88 \pm 0.70_{a,B}$	$87.85 \pm 0.52_{g,C}$	$12.15 \pm 0.52_{b,A}$	$57.08 \pm 0.45_{f,A}$	$42.92 \pm 0.45_{b,C}$
72	$53.85 \pm 0.42_{e,B}$	$46.15 \pm 0.42_{b,c,B}$	$85.72 \pm 0.21_{f,C}$	$14.28 \pm 0.21_{c,A}$	$51.24 \pm 0.42_{e,A}$	$48.76 \pm 0.42_{c,C}$
96	$53.28 \pm 0.31_{e,B}$	$46.72 \pm 0.31_{c,B}$	$85.72 \pm 0.15_{f,C}$	$14.28 \pm 0.15_{c,A}$	$47.12 \pm 0.49_{c,d,A}$	$52.88 \pm 0.49_{d,e,C}$
144	$50.73 \pm 0.25_{d,B}$	$49.27 \pm 0.25_{d,B}$	$84.06 \pm 0.38_{e,C}$	$15.94 \pm 0.38_{d,A}$	$47.89 \pm 0.30_{d,A}$	$52.11 \pm 0.30_{d,C}$
168	$49.22 \pm 0.29_{d,B}$	$50.78 \pm 0.29_{d,B}$	$81.37 \pm 0.27_{d,C}$	$18.63 \pm 0.27_{e,A}$	$45.22 \pm 0.15_{c,A}$	$54.78 \pm 0.15_{e,C}$
192	$46.80 \pm 0.53_{c,A}$	$53.20 \pm 0.53_{e,B}$	$81.97 \pm 0.19_{d,B}$	$18.03 \pm 0.19_{e,A}$	$46.30 \pm 0.35_{cd,A}$	$53.70 \pm 0.35_{d,e,B}$
240	$55.34 \pm 1.65_{a,B}$	$44.66 \pm 1.65_{b,B}$	$77.52 \pm 0.54_{c,C}$	$22.48 \pm 0.54_{f,A}$	$42.49 \pm 0.61_{b,A}$	$57.51 \pm 0.61_{f,C}$
336	$42.99 \pm 0.57_{b,B}$	$57.01 \pm 0.57_{f,B}$	$69.77 \pm 0.75_{a,C}$	$30.23 \pm 0.75_{h,A}$	$39.12 \pm 0.67_{a,A}$	$60.88 \pm 0.67_{g,C}$
480	$40.58 \pm 0.26_{a,A}$	$59.42 \pm 0.26_{g,B}$	$71.25 \pm 0.58_{b,B}$	$29.75 \pm 0.58_{h,A}$	$39.78 \pm 0.45_{a,A}$	$60.22 \pm 0.45_{g,B}$
EY (%)	$73.84 \pm 1.51_{A}$		$88.14 \pm 1.64_{B}$		$91.02 \pm 1.48_{B}$	
Loss of total iron in W_1 (%)	$36.0 \pm 0.53_{B}$		$22.2 \pm 0.35_{A}$		$66.3 \pm 0.42_{C}$	

Values in the same column bearing different small case letters are significantly different ($P < 0.05$). Values in the same row bearing different capital letters are significantly different ($P < 0.05$).

Coacervate yield was not only affected by the total concentration of the biopolymers used, but also by the ratio between the biopolymers. In Fig. 4, it is observed that the maximum coacervate yield was obtained using a Pr:Ps ratio equal to 2:1 for WPC:MG at pH_E, similar results were found for WPC:GA and WPC:LMP binary mixtures (data not shown). This ratio was confirmed experimentally by determining the chemical equivalents of each biopolymer by titration with 0.1N NaOH, being 0.7 mEq/g for WPC, 1.4 mEq/g for GA, 1.35 mEq/g for GM, and 1.3 mEq/g for LMP.

The GA, MG and LMP concentration in the coacervates was determined by elemental analysis and used as an indicative of coacervates yield. Maximum polysaccharides concentration in the coacervates (data not shown) was obtained at pH_c, total biopolymers concentrations of 5% for WPC–GA and WPC–MG, and 0.7% for WPC–LMP, and a biopolymer ratio of 2:1, agreeing with the results given above.

3.3. Characterization of the $(W_1/O/W_2)_{a,b,c}$ multiple emulsions

All the multiple emulsions formed were type C systems (Fig. 5) where most of the multiple emulsion droplets contain a substantial number of inner droplets; the inner droplets in a type C emulsion are usually flocculated and rather close-packed (Dickinson & McClements, 1996). The binary biopolymer mixtures affected significantly the $d_{3,0}$, and the span of the freshly prepared $(W_1/O/W_2)_{a,b,c}$ multiple emulsions, and in consequence in the $K_{C(W1/O/W2)a,b,c}$ (Table 2). The $(W_1/O/W_2)_{5\%,2:1,WPC:MG}$ multiple emulsion exhibited significantly lower initial $d_{3,0}$, span and $K_{C(W1/O/W2)}$ followed by the $(W_1/O/W_2)_{5\%,2:1,WPC:GA}$, and by the $(W_1/O/W_2)_{0.7\%,2:1,WPC:LMP}$ multiple emulsions, respectively. Thus, an initial lower span value combined with a smaller droplet size in the fresh emulsions, resulted in emulsions that showed a greater stability, i.e., a lesser change in their droplet size per unit volume with aging time (Fig. 6). Food emulsions normally contain a range of different droplet sizes and the larger droplets tend to cream more rapidly than the smaller droplets, so that there is a distribution of creaming rates within the emulsion, with the net result that there is both a droplet concentration profile and a droplet size profile in the vertical direction within an emulsion. As the larger droplets move upward more rapidly they collide with smaller droplets (McClements, 2005), forming three-dimensional droplets aggregates that eventually coalesce and destabilize the emulsions.

Table 4
Z-average diameter of Pr:Ps complexes.

Pr:Ps complex	Z-average diameter (nm)
WPC:GA	484.90 ± 0.45 b
WPC:GM	529.40 ± 0.49 c
WPC:LMP	398.10 ± 0.36 a

Values bearing different letters are significantly different ($P < 0.05$).

3.4. Protective effect of the $(W_1/O/W_2)_{a,b,c}$ multiple emulsions against ferrous bisglycinate oxidation

All the $(W_1/O/W_2)_{a,b,c}$ multiple emulsions showed a significant decrease in their Fe^{2+} content with storage time (Table 3). $(W_1/O/W_2)_{5\%,2:1,WPC:MG}$ emulsion presented the smallest difference between the initial and final Fe^{2+} content, followed by the $(W_1/O/W_2)_{5\%,2:1,WPC:GA}$ and $(W_1/O/W_2)_{0.7\%,2:1,WPC:LMP}$ multiple emulsions, respectively. The $(W_1/O/W_2)_{0.7\%,2:1,WPC:LMP}$ showed a non-significant different initial Fe^{+2} content from the $(W_1/O/W_2)_{5\%,2:1,WPC:MG}$ multiple emulsion, but it was the one that suffered the most drastic Fe^{2+} content decrease with storage time (92.0%–39.78%). On the other hand, the $(W_1/O/W_2)_{5\%,2:1,WPC:GA}$ multiple emulsion entrapped a significantly initial lower amount of Fe^{+2}, but its Fe^{+2}

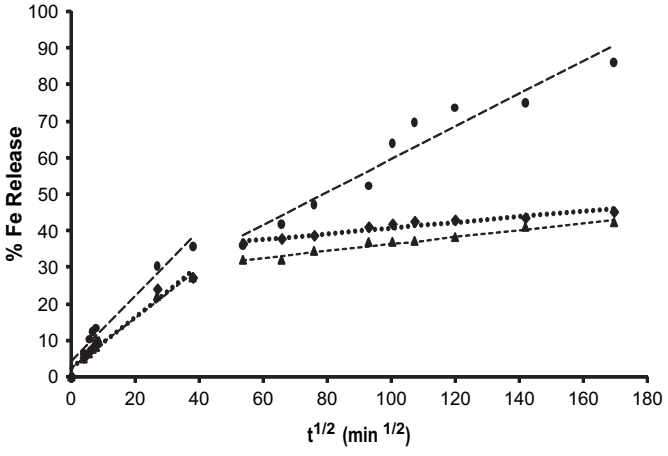

Fig. 7. Theoretically predicted (using Higuchi's model; discontinuous lines) and experimental data of ferrous bisglycinate release from W_1 to W_2 in: a) $(W_1/O/W_2)_{5\%,2:1,WPC:GA}$ (……; ◆), b) $(W_1/O/W_2)_{5\%,2:1,WPC:GM}$ (– – –; ▲), and c) $(W_1/O/W_2)_{5\%,2:1,WPC:LMP}$ (— —; ●) multiple emulsions.

Table 5
Kinetic parameters of release of ferrous bisglycinate from W_1 to W_2 phases of $(W_1/O/W_2)_{a,b,c}$ multiple emulsions during the first 24 h and after 24 h for each kinetic model tested.

	Kinetic parameters of release from multiple emulsions (first 24 h)					
	$(W_1/O/W_2)_{5\%,\ 2:1,WPC:GA}$	R^2	$(W_1/O/W_2)_{5\%,\ 2:1,WPC:MG}$	R^2	$(W_1/O/W_2)_{0.7\%,\ 2:1,WPC:LMP}$	R^2
K_{HC} (min^{-1})	2.00×10^{-4}	0.18	2.00×10^{-4}	0.11	3.00×10^{-4}	0.16
K_{PH} (min^{-2})	4.40×10^{-2}	0.66	5.20×10^{-2}	0.46	8.00×10^{-2}	0.60
K_J (min^{-1})	4.60×10^{-1}	0.68	9.00 × 10-1	0.74	1.60×10^{1}	0.70
K_0 (mg mL^{-1} min^{-1})	1.68×10^{-2}	0.85	1.64×10^{-2}	0.88	2.14×10^{-2}	0.84
K_1 (min^{-1})	1.10×10^{-3}	0.82	1.10×10^{-3}	0.84	1.00×10^{-3}	0.78
K_2(mL mg^{-1} min^{-1})	-9.00×10^{-5}	0.69	-9.00×10^{-5}	0.67	-6.00×10^{-5}	0.56
K_H (mg mL^{-1} $min^{-0.5}$)	7.02×10^{-1}	0.97	6.88×10^{-1}	0.98	8.99×10^{-1}	0.96
Kinetic parameters of release from multiple emulsions (after 24 h)						
K_{HC} (min^{-1})	7.00×10^{-6}	0.39	9.00×10^{-6}	0.86	3.00×10^{-5}	0.78
K_{PH} (min^{-2})	1.40×10^{-1}	0.69	1.70×10^{-1}	0.83	5.00×10^{-1}	0.90
K_J (min^{-1})	2.40×10^{-3}	0.49	2.60×10^{-3}	0.82	2.40×10^{-3}	0.89
K_0 (mg mL^{-1} min^{-1})	4.00×10^{-4}	0.90	3.00×10^{-4}	0.82	1.90×10^{-3}	0.85
K_1 (min^{-1})	1.00×10^{-5}	0.87	8.00×10^{-6}	0.80	3.00×10^{-5}	0.85
K_2(mL mg^{-1} min^{-1})	-3.00×10^{-7}	0.85	-2.00×10^{-7}	0.78	-6.00×10^{-7}	0.79
K_H (mg mL^{-1} $min^{-0.5}$)	9.43×10^{-2}	0.96	7.46×10^{-2}	0.92	4.46×10^{-1}	0.93

K_{HC}, K_{PH}, K_J, K_0, K_1, K_2, and K_H are the release rate constants for: Hixson & Crowell, Peppas-Higuchi, Jorgensen & Christensen, zero-order, first-order, second-order, and Higuchi's model respectively.

content was non-significantly lower than that of the $(W_1/O/W_2)_{0.7\%,2:1,WPC:LMP}$ multiple emulsion at the end of the storage time (Table 3). These results suggest that both the Fe^{2+} entrapment capacity and the protection against the oxidation of ferrous bisglycinate were dependent of the type of polysaccharide used in the Pr:Ps complex forming the outer interfacial membrane of the multiple emulsions. A significantly higher protection against ferrous bisglycinate oxidation was provided by the $(W_1/O/W_2)_{5\%,2:1,WPC:MG}$ than the $(W_1/O/W_2)_{5\%,2:1,WPC:GA}$ multiple emulsion, despite that GA and MG have similar chemical composition and physicochemical characteristics (Vernon-Carter et al., 2000). It has been reported that MG has a considerably greater molecular weight (~2, 120, 000 Da) (Vernon-Carter, Pedroza-Islas, & Beristain, 1998) than GA (≤1, 000, 000 Da) (Fenyo & Vandevelde, 1990), which is in agreement with results of z-average diameter of the Pr:Ps complexes presented in Table 4, so that it is probable that the adsorbed layer around the multiple emulsion containing MG is thicker than that containing GA, and that the resistance opposing the diffusion of pro-oxidant agents is directly proportional to the adsorbed biopolymer membrane thickness. The $(W_1/O/W_2)_{0.7\%,2:1,WPC:LMP}$ multiple emulsion provided the worst protection against Fe^{+2} oxidation, and these results tend to confirm that the thickness of the adsorbed biopolymer layer might be in great measure responsible for providing protection to Fe^{2+} against oxidation, as LMP had the lowest molecular weight (~150, 000 Da) among the three polysaccharides used and the WPC:LMP complex zeta-average diameter was the smallest among the three complexes used in this study. Adsorbed layer thickness seems to be also the main factor affecting multiple emulsion stability against coalescence. The greater the molecular weight of the polysaccharide making up the Pr:Ps complex, the greater the adsorbed layer thickness, the greater the steric repulsion forces (McClements, 2005), the lower the ($K_{C\ (W1/O/W2)a,b,c}$) values, and the higher the multiple emulsion stability (Table 2).

3.4.1. Encapsulation yield and release kinetics

The EY of the $(W_1/O/W_2)_{a,b,c}$ multiple emulsions is shown in Table 3. The results for EY were very similar and followed the same tendencies as that displayed by the Fe^{2+} concentrations the $(W_1/O/W_2)_{a,b,c}$ multiple emulsions, i.e., that the $(W_1/O/W_2)_{5\%,2:1,WPC:MG}$ and $(W_1/O/W_2)_{0.7\%,2:1,WPC:LMP}$ multiple emulsions showed non-significant differences in EY between themselves, but significantly higher EY than the $(W_1/O/W_2)_{5\%,2:1,WPC:GA}$ multiple emulsion. The amount of total iron within W_1 for each $(W_1/O/W_2)_{a,b,c}$ multiple emulsion diminished significantly in all cases with storage time as follows: 22.2% for $(W_1/O/W_2)_{5\%,2:1,WPC:MG}$, 36.0% for $(W_1/O/W_2)_{5\%,2:1,WPC:GA}$, and 66.3% for $(W_1/O/W_2)_{0.7\%,2:1,WPC:LMP}$, respectively, probably because the portion of iron that was released into W_2 was oxidized.

Experimental release curves of the ferrous bisglycinate from the $(W_1/O/W_2)_{a,b,c}$ multiple emulsions are given in Fig. 7. Fitting of the experimental data to Hixson & Crowell, Peppas-Higuchi, Jorgensen & Christensen, zero, first and second-order kinetics provided relatively low correlation coefficients (R^2 ranged in between 0.11 and 0.90), probably because the data seemed to follow a global release process that occurred in two consecutive single processes with different release kinetic rates: (1) An initial stage characterized by a steep gradient induced by the relatively high initial total iron concentration in the interior of W_1 compared to its concentration in W_2, which took place at short storage times (~24 h), and (2) a second stage occurring at storage times larger than 24 h, where the gradient drastically diminished, probably because the concentrations in total iron between W_1 and W_2 tended to equilibrium. The data of both the steep and the relatively flat gradient stages of Fig. 7 were fitted to Higuchi's model (Higuchi, 1961), obtaining high correlation coefficients (R^2 from 0.92 to 0.98) (Table 5). Higuchi's release kinetics constants (K_H) for the steep gradient stage were from lower to higher as follows: 0.69 mg mL^{-1} $min^{-0.5}$ for $(W_1/O/W_2)_{5\%,2:1,WPC:MG}$, 0.70 mg mL^{-1} $min^{-0.5}$ for $(W_1/O/W_2)_{5\%,2:1,WPC:GA}$, and 0.90 mg mL^{-1} $min^{-0.5}$ for $(W_1/O/W_2)_{0.7\%,2:1,WPC:LMP}$, and for the second relatively flat gradient stage were 0.07 mg mL^{-1} $min^{-0.5}$ for $(W_1/O/W_2)_{5\%,2:1,WPC:MG}$, 0.09 mg mL^{-1} $min^{-0.5}$ for $(W_1/O/W_2)_{5\%,2:1,WPC:GA}$, and 0.45 mg mL^{-1} $min^{-0.5}$ for $(W_1/O/W_2)_{0.7\%,2:1,WPC:LMP}$, respectively. These results seem to indicate and confirm that release kinetics of ferrous bisglycinate from the inner aqueous phase of the multiple emulsions to the outer aqueous phase is highly dependent on the length of the diffusion pathways, i.e. the thicker the Pr:Ps complex interfacial membrane thickness in the $(W_1/O/W_2)_{a,b,c}$ multiple emulsions, the slower the release kinetics.

4. Conclusions

In this work a methodology and the general guidelines for achieving an efficient encapsulation, enhancing the protection against oxidation and controlling the rate of release of ferrous

bisglycinate from water-in-oil-in-water multiple emulsions stabilized with protein:polysaccharides complexes was established. Given that ferrous deficiency is the most common nutritional deficiency in both the industrialized and developing worlds, affecting mostly infants, children, and women of childbearing age, we hope that this work helps to mitigate this problem.

Acknowledgements

The authors wish to thank the Consejo Nacional de Ciencia y Tecnologia (CONACyT) of Mexico for partially financing this project through grant U-81157-Z.

References

AOAC Official Methods of Analysis. (1995). *AOAC official method 977.30. Iron in drugs, spectrophotometric method*. Drugs part I, (pp. 11–12). Arlington: AOAC International.

Bais, D., & Lapasin, R. (2003). Studio di matrici polisaccharidiche per emulsioni: interazioni polimero tensioattivo e propietà reologiche. *Rivista Italiana delle Sostanze Grasse, 80*, 129–139.

Benichou, A., Aserin, A., & Garti, N. (2002). Double emulsions stabilized by new molecular recognition hybrids of natural polymers. *Polymers for Advanced Technologies, 13*, 1019–1031.

Bergenståhl, B. (1995). Emulsions. In S. T. Becket, & G. Talbot (Eds.), *Physico-chemical aspects of food processing* (pp. 49–64). London: Chapman & Hall.

Bonnet, M., Cansell, M., Berkaoui, A., Ropers, M. H., Anton, M., & Leal-Calderon, F. (2009). Release rate profiles of magnesium from multiple W/O/W emulsions. *Food Hydrocolloids, 23*, 92–101.

Bovell-Benjamin, A. C., Viteri, F. E., & Allen, L. H. (2000). Iron absorption from ferrous bisglycinate and ferric trisglycinate in whole maize is regulated by iron status. *The American Journal of Clinical Nutrition, 71*, 1563–1569.

Dickinson, E. (2008). Interfacial structure and stability of food emulsions as affected by protein–polysaccharide interactions. *Soft Matter, 4*, 932–942.

Dickinson, E., & McClements, D. J. (1996). *Advances in food colloids*. London: Blackie Academic & Professional.

Espinosa-Andrews, H., Báez-González, J. G., Cruz Sosa, F., & Vernon-Carter, E. J. (2007). Gum arabic-chitosan complex coacervation. *Biomacromolecules, 8*, 1313–1318.

Ettelaie, R., Akinshina, A., & Dickinson, E. (2008). Mixed protein–polysaccharide interfacial layers: a self consistent field calculation study. *Faraday Discussions, 139*, 161–178.

Fenyo, J. C., & Vandevelde, M. C. (1990). Physico-chemical properties of gum Arabic in relation to structure. In G. O. Phillips, D. J. Wedlock, & P. A. Williams (Eds.), *Gums and stabilizers for the food industry, Vol. 5* (pp. 17–23). Oxford: IRL Press.

Higuchi, T. (1961). Rate of release of medicaments from ointment bases containing drugs in suspension. *Journal of Pharmaceutical Sciences, 50*, 874–879.

Kitchener, J. A., & Mussellwhite, P. R. (1969). The theory of stability of emulsions. In Sherman. (Ed.), *Emulsion science* (pp. 77–130). London: Academic Press Inc.

Kralj, D., & Brečević, L. (1998). Precipitation of some slightly soluble salts using emulsion liquid membranes. *Croatian Chemical Acta, 71*, 1049–1060.

Lobato-Calleros, C., Rodriguez, E., Sandoval-Castilla, O., Vernon-Carter, E. J., & Alvarez-Ramirez, J. (2006). Reduced-fat white fresh cheese-like products obtained from $W_1/O/W_2$ multiple emulsions: viscoelastic and high-resolution image analyses. *Food Research International, 39*, 678–685.

Lobato-Calleros, C., Sosa-Pérez, A., Rodríguez-Tafoya, J., Sandoval-Castilla, O., Pérez-Alonso, C., & Vernon-Carter, E. J. (2008). Structural and textural characteristics of reduced-fat cheese-like products made from $W_1/O/W_2$ emulsions and skim milk. *LWT – Food Science and Technology, 41*, 1847–1856.

Lutz, R., Aserin, A., Portnoy, Y., Gottlieb, M., & Garti, N. (2009). On the confocal images and the rheology of whey protein isolated and modified pectins associated complex. *Colloids and Surfaces B: Biointerfaces, 69*, 43–50.

McClements, D. J. (2005). *Food emulsions. Principles, practices, and techniques*. Boca Raton, Florida: CRC Press.

Muschiolik, G. (2007). Multiple emulsions for food use. *Current Opinion in Colloid and Interface Science, 12*, 213–220.

Pasika, W. M. (1977). Polysaccharide polyelectrolites. In P. A. Sanford, & A. I. Laskin (Eds.), *Extracellular microbial polysaccharides, Vol. 45* (pp. 128–159). Washington, DC: ACS Symposium Series.

Pimentel-González, D., Revah, S., Campos-Montiel, R., Monroy-Hermosillo, O., & Vernon-Carter, E. J. (2008). A laboratory study of the biodegradation of MTBE solubilised in water by a microbial consortium entrapped in a water-in-oil-in-water double emulsion. *Process Biochemistry, 43*, 1239–1243.

Rodríguez-Huezo, M. E., Pedroza-Islas, R., Prado-Barragán, L. A., Beristain, C. I., & Vernon-Carter, E. J. (2004). Microencapsulation by spray drying of multiple emulsions containing carotenoids. *Journal of Food Science, 69*, E351–E359.

Ruíz-Ramos, J. O., Pérez-Orozco, J. P., Báez-González, J. G., Bósquez-Molina, E., Pérez-Alonso, C., & Vernon-Carter, E. J. (2006). Interrelationship between the viscoelastic properties and effective moisture diffusivity of emulsions with the water vapor permeability of edible films stabilized by mesquite gum–chitosan complexes. *Carbohydrate Polymers, 64*, 355–363.

Tolstoguzov, Y. B. (1990). Interactions of gelatin with polysaccharides. In G. O. Phillips, D. J. Wedlock, & P. A. Williams (Eds.), *Gums and stabilisers for the food industry 5* (pp. 157–175). Oxford: IRL Press.

Tolstoguzov, Y. B. (1998). Functional properties of protein–polysaccharide mixtures. In S. E. Hill, D. A. Ledward, & J. R. Mitchell (Eds.), *Functional properties of food macromolecules* (pp. 252–277). Gaithersburg: Aspen Publishers.

Vernon-Carter, E. J., Beristain, C. I., & Pedroza-Islas, R. (2000). Mesquite gum (*Prosopis gum*). In G. Doxastasis, & V. Kiosseoglou (Eds.), *Novel macromolecules in food systems* (pp. 217–235). Amsterdam: Elsevier.

Vernon-Carter, E. J., Gómez, S. A., Beristain, C. I., Mosqueira, G., Pedroza-Islas, R., & Moreno-Terrazas, R. C. (1996). Color degradation and coalescence kinetics of Aztec marigold oleoresin-in-water emulsions stabilized by mesquite or arabic gums and their blends. *Journal of Texture Studies, 27*, 625–641.

Vernon-Carter, E. J., Pedroza-Islas, R., & Beristain, C. I. (1998). Stability of *Capsicum annum* oleoresin-in water emulsions containing *Prosopis* and *Acacia* gums. *Journal of Texture Studies, 29*, 553–567.

Voragen, A. G. J., Pilnik, W., Thibault, J. F., Axelos, M. A. V., & Renard, C. M. G. C. (1995). Pectins. In A. M. Stephen (Ed.), *Food polysaccharides and their applications* (pp. 287–339). New York: Marcel Dekker, Inc.

Weinbreck, F., Nieuwenhuijse, H., Robjin, G. W., & de Kruif, C. G. (2003). Complex formation of whey proteins: exocellular polysaccharide EPS B40. *Langmuir, 19*, 9404–9410.

Weinbreck, F., Tromp, R. H., & de Kruif, C. G. (2004). Composition and structure of whey protein/gum arabic coacervates. *Biomacromolecules, 5*, 1437–1445.

Weinbreck, F., Wientjes, R. H. W., Nieuwenhuijse, H., Robjin, G. W., & de Kruif, C. G. (2004). Rheological properties of whey protein/gum arabic coacervates. *Journal of Rheology, 48*, 1215–1228.